

Nanocomposite Fiber Systems Processed from Fluorinated Single-Walled Carbon Nanotubes and a Polypropylene Matrix

Daneesh McIntosh,[†] Valery N. Khabashesku,^{*,‡} and Enrique V. Barrera^{*,†}

Department of Mechanical Engineering and Materials Science, Department of Chemistry, and Richard E. Smalley Institute for Nanoscale Science and Technology, Rice University, Houston, Texas 77005-1892

Received March 2, 2006. Revised Manuscript Received June 22, 2006

Processing composites of carbon nanotubes into nanotube continuous fibers (NCFs) is an effective way of manipulating the anisotropic properties of the single-walled carbon nanotubes (SWNTs) as it becomes less difficult to transform the SWNTs into an aligned configuration when they are confined in a small diameter fiber. This helps to take fuller advantage of the high mechanical properties of the SWNT materials in the axial direction. However, in creating nanocomposite fiber systems, the issues of dispersion and nanotube–matrix interaction and adhesion become of utmost importance when improved mechanical properties are anticipated. In addressing these issues in this work it has been found that sidewall chemical functionalization can be an effective tool for improving both the dispersion and interaction between the nanotube and the matrix. This work evaluates the effect of sidewall functional groups on fluorinated single-walled carbon nanotubes (F-SWNTs) as a precursor for improved interfacial adhesion in a thermoplastic matrix (polypropylene, PP) via partial defluorination of the F-SWNTs. The partial removal of functional groups from the F-SWNTs during melt processing with PP by shear mixing provides the opportunity for in situ direct covalent bonding between the nanotubes and the matrix during melt processing which ultimately results in better mechanical reinforcement of the composite. The studies conducted herein demonstrate that in comparison with PP composites filled with purified nanotubes (P-SWNTs), improved dispersion, interfacial adhesion, and mechanical properties are achieved for F-SWNT-loaded matrixes due to chemical functionalization.

Introduction

Small diameter nanocomposite fiber systems can be used to effectively manipulate the orientation of nanoparticles such as carbon nanotubes in polymer matrixes. The fiber spinning process in which the molten composite is drawn to smaller diameters at higher take-up speeds is exploited in manufacturing our nanotube continuous fibers (NCFs). The reduced diameter fiber is used to align the carbon nanotubes such that the majority of the nanotubes or their ropes are preferentially elongated along the length of the fiber. Pötschke et al.¹ showed this type of alignment in multiwalled carbon nanotubes in a polycarbonate matrix after melt spinning.

Carbon nanotubes have been used as the choice of reinforcement in several composite fiber systems, exploiting not only the level of alignment that can be achieved but also the fact carbon nanotubes have superior mechanical properties despite their nanoscopic proportions. Several researchers have reported improved mechanical properties for composites incorporating single-walled carbon nanotubes (SWNTs). Min et al.² have reported improved mechanical properties of the

polyacrylonitrile/SWNT composite fibers studied, their composite fibers showing 43, 105, and 16% increases in tensile strength, tensile modulus, and strain to failure, respectively. Zhang et al.³ reported a 40% increase in the elastic modulus of the poly(vinyl alcohol)/SWNT composite fibers produced via gel spinning. Kearns and Shambaugh⁴ reported a 40% increase in fiber tensile strength for composites of polypropylene (PP) and 1 wt % loading of SWNTs. Moore et al.⁵ also studied a similar fiber composite system. Kumar et al.,⁶ however, report a 60% increase in tensile strength and a 20% increase in tensile modulus for poly(*p*-phenylene benzobisoxazole) (PBO)/SWNT fiber composites generated from an in situ polymerization of PBO in poly(phosphoric acid) in the presence of SWNTs.

Our studies move one step further in not only manufacturing a fiber system but also incorporating higher weight percentages of carbon nanotubes in a PP matrix wherein the carbon nanotubes are covalently attached to the surrounding polymer via an in situ reaction initiated during the melt spinning process. The supporting principle for this was

* To whom correspondence should be addressed. E-mail: khval@rice.edu (V.N.K.); ebarrera@rice.edu (E.V.B.).

[†] Department of Mechanical Engineering and Materials Science.

[‡] Department of Chemistry and Richard E. Smalley Institute for Nanoscale Science and Technology.

(1) Pötschke, P.; Brünig, H.; Janke, A.; Fischer, D.; Jehnichen, D. *Polymer* **2005**, *46*, 10355.

(2) Min, B. G.; Sreekumar, T. V.; Uchida, T.; Kumar, S. *Carbon* **2005**, *43*, 599.

(3) Zhang, X.; Liu, T.; Sreekumar, T. V.; Kumar, S.; Hu, X.; Smith, K. *Polymer* **2004**, *45*, 8801

(4) Kearns, J. C.; Shambaugh, R. L. *J. Appl. Polym. Sci.* **2002**, *86*, 2079.

(5) Moore, E. E.; Ortiz, D. L.; Marla, V. T.; Shambaugh, R.L.; Grady, B. P. *J. Appl. Polym. Sci.* **2004**, *93*, 2926.

(6) Kumar, S.; Dang, T. D.; Arnold, F. E.; Bhattacharyya, A. R.; Min, B. G.; Zang, X. F. *Macromolecules* **2002**, *35*, 9039.

presented by Shofner et al.⁷ in their studies incorporating F-SWNT in polyethylene. They proposed the reaction scheme in which the loss of a fluorine moiety during the melt processing stage acts as a catalyst for the subsequent linkage of the nanotube to the surrounding polymer matrix. In comparison with the previous study,⁷ in case of PP/F-SWNT composite system an enhanced chemical interaction was expected due to the presence of more reactive tertiary C–H bonds in PP structure and a higher melt processing temperature. Also, PP was chosen as the polymer matrix in our NCF systems because it is a thermoplastic material that, for general wider-scale applications, has excellent chemical resistance and superior mechanical properties compared to similar classes of polymer. Tensile strengths in the range 30–38 MPa and tensile moduli ranging from 1.1 to 1.6 GPa for bulk PP materials have been reported.⁸ Despite the good mechanical properties of this polymer, efforts to improve them even further have been undertaken through incorporation of many varied types of fillers and reinforcements such as glass fiber, mica, talc, and calcium carbonate.^{9–12} Conventional short fibers such as aramid, carbon, and varied natural fibers have also been used as reinforcements in the thermoplastic polymeric matrix, each with the main objective of improving the mechanical properties of the polymer. The nonpolar nature of PP often makes the incorporation of fillers and reinforcements, which tend to be polar in nature, very difficult resulting in weak adhesion between the filler surface and the polymer matrix. In these cases, poor wetting of the filler or reinforcement by the polymer causes agglomerations of the filler particles generally resulting in poor dispersion and insufficient reinforcement by the filler particle.

To achieve maximum adhesion of the filler to the polymer matrix, the fillers can be exposed to surface treatments rendering them more hydrophilic. Examples of these treatments include exposure to stearic acid and other additives such as silanes, zirconates, and titanates.¹³ These materials interact with both the filler surface and the polymer to increase adhesion between the two. In our studies fluorinated single-walled carbon nanotubes (F-SWNTs) are chosen as the filler or reinforcement material. Enhanced interaction at the interface with the polymer matrix results from the separation of fluorine moieties from the F-SWNTs during processing, which initiates a free radical reaction resulting in the formation of a covalent bond with the surrounding polymer matrix. This stronger interfacial adhesion facilitates better load transfer when the material is subjected to mechanical loading.

The materials used in this study were each chosen to exploit not only the processing procedure but also the

inherent material properties. High molecular weight isotactic PP was used to take advantage of the high crystallinity that can be achieved with the ordering of the molecular chains, especially when the small diameter fiber composites are generated. NCFs with varying weight percents of functionalized and purified single-walled carbon nanotubes (P-SWNTs) were incorporated into the form of a continuous fiber, which helps to harness the high mechanical properties of the nanotube-reinforcing element while maintaining the flexibility of the overall system allowing for better handling for macroscopic applications. Individual SWNTs have tensile strengths in the range 20–200 GPa and an elastic modulus approaching 1 TPa¹⁴ and would be preferentially used as nanosize reinforcements in the polymer matrix. SWNTs are, however, more likely to be incorporated in the matrix as ropes or bundles of nanotubes as a result of van der Waals forces that hold many entangled ropes together. These ropes or bundles are reported as having tensile strengths in the range of 15–52 GPa.^{15–17} In many composite systems, roping and the chemically inert structure of SWNTs can hamper load transfer to the SWNTs, limiting the mechanical property improvements in the composite systems generated. These ropes generally have diameters that are 1 or 2 orders of magnitude larger than an individual SWNT and lengths of several micrometers.¹⁸ Ineffective interfacial bonding and sliding of individual nanotubes within the ropes inhibit load transfer from the matrix to the fiber, limiting the amount of mechanical reinforcement achievable in polymer matrix composites.¹⁹ Individual nanotubes are expected to provide the most reinforcement. Functionalization of the nanotube surface via fluorination was shown to be a method to introduce reactive moieties, to disrupt the rope structure, and to obtain smaller diameter ropes and possibly individual nanotubes.²⁰ Functionalization, in general, can be used for a variety of purposes such as separating nanotubes by type (e.g., semiconducting vs metallic),²¹ improving the solubility of nanotubes,^{22–30} or dispersion of functionalized nanotubes in composites. The latter contributes to increased mechanical

- (7) Shofner, M.; Khabashesku, V. N.; Barrera, E. V. *Chem. Mater.* **2006**, *18*, 906.
 (8) Hertzberg, R. W. *Deformation and Fracture Mechanics of Engineering Materials*, 4th ed.; John Wiley and Sons: New York, 1996.
 (9) Liu, X.; Wu, Q. *Polymer* **2001**, *42*, 10013.
 (10) Velasco, J. I.; De Saja, J. A.; Martinez, A. B. *J. Appl. Polym. Sci.* **1996**, *61*, 125.
 (11) Chiang, W. Y.; Yang, W. D.; Pukanszky, B. *Polym. Eng. Sci.* **1994**, *34*, 485.
 (12) Kuhnert, I.; Fisher, H. D.; Muras, J. *Kunststoff* **1997**, *42*, 29.
 (13) Karian, H. G. *Handbook of Polypropylene and Polypropylene Composites*, 2nd ed.; Marcel Dekker: New York, 2003.

- (14) Krishnan, A.; Dujardin, E.; Ebbesen, T. W.; Yianilos, P. N.; Treacy, M. M. *J. Phys. Rev. B* **1998**, *58*, 14013.
 (15) Shenderova, O. A.; Zhirnov, V. V.; Brenner, D. W. *Crit. Rev. Solid State Mater. Sci.* **2002**, *27*, 227.
 (16) Treacy, M. M. J.; Ebbesen, T. W.; Gibson, J. M. *Nature* **1996**, *381*, 678.
 (17) Lourie, O.; Cox, D. M.; Wagner, H. D. *Phys. Rev. Lett.* **1998**, *81*, 1638.
 (18) Thess, A.; Lee, R.; Nikolaev, P.; Dai, H.; Petit, P.; Robert, J.; Xu, C.; Lee, Y. H.; Kim, S. G.; Rinzler, A. G.; Colbert, D. T.; Scuseria, G. E.; Tomanek, D.; Fischer, J. E.; Smalley, R. E. *Science* **1996**, *273*, 483.
 (19) Ajayan, P. M.; Schadler, L. S.; Giannaris, C.; Rubio, A. *Adv. Mater.* **2000**, *12*, 750.
 (20) Khabashesku, V. N.; Billups, W. E.; Margrave, J. L. *Acc. Chem. Res.* **2002**, *35*, 1087.
 (21) Dyke, C. A.; Stewart, M. P.; Tour, J. M. *J. Am. Chem. Soc.* **2005**, *127*, 4498.
 (22) Boul, P. J.; Liu, J.; Mickelson, E. T.; Huffman, C. B.; Ericson, L. M.; Chiang, I. W.; Smith, K. A.; Colbert, D. T.; Hauge, R. H.; Margrave, J. L.; Smalley, R. E. *Chem. Phys. Lett.* **1999**, *310*, 367.
 (23) Bahr, J. L.; Tour, J. M. *Chem. Mater.* **2001**, *13*, 3823.
 (24) Chen, Y.; Haddon, R. C.; Fang, S.; Rao, A. M.; Eklund, P. C.; Lee, W. H.; Dickey, E. C.; Grulke, E. A.; Pendergrass, J. C.; Chavan, A.; Haley, B. E.; Smalley, R. E. *J. Mater. Res.* **1998**, *13*, 2423.
 (25) Georgakilas, V.; Kordatos, K.; Prato, M.; Guldi, D. M.; Holzinger, M.; Hirsch, A. *J. Am. Chem. Soc.* **2002**, *124*, 760.

properties which have been observed in several published works.^{7,31,32}

This paper describes the use of SWNTs, surface-functionalized by fluorine moieties (F-SWNTs), to address the problems of both dispersion and interaction between the nanotube and the matrix in the composite system. The processing, nanotube/matrix interaction, mechanical properties, and alignment of the nanotubes within the PP matrix, containing functionalized and pristine SWNTs, respectively, are also examined. The analysis shows that the fluorine functional groups enhance the interaction with PP, improve the dispersion of nanotubes in the matrix, and increase the mechanical properties when compared to the composites containing P-SWNTs or the neat PP. It is proposed that fluorine atoms, formed during thermal dissociation of C–F moieties on the F-SWNTs under mechano-chemical processing conditions, attack the PP chain to scavenge hydrogen and form HF and radical sites, creating an opportunity for grafting of the polymer to the nanotube surface via direct covalent bonding. The presented results thus demonstrate a new method for in situ design of fully integrated nanotube composites.³³

Experimental Section

Materials. The purified and fluorinated HiPco SWNTs, used in the present work, were purchased from Carbon Nanotechnologies, Inc. (batch numbers D0310 and F0219-1, respectively). The PP samples were made from isotactic PP with $M_n = 67\,000$ and $M_w = 250\,000$ with a melt index of 12 g/10 min (230 °C/2.16 kg, ASTM D1238) as obtained from Aldrich Chemicals. The PP composite samples were produced in 20 g batches that contained varying weight percent loads of P-SWNT and F-SWNT.

Composites Fabrication. To fabricate the composite materials from the two components, F-SWNTs or P-SWNTs, and PP, a multistep processing procedure was used. The steps included dispersion of SWNTs into solvent to disrupt large agglomerates, incipient wetting of the polymer, and high shear mixing, followed by pelletization and fiber spinning. The final product resulting from these processing and fabrication steps was NCFs with diameters of approximately 130 μm .

In the initial stages of processing, each load of either P-SWNTs or F-SWNTs was combined with a solvent to create a suspension. Low boiling point solvents were used for this study so the solvent can be evaporated in a later stage without melting the polymer. The P-SWNT suspensions were prepared by sonication for several minutes in chloroform, while the F-SWNT suspensions were

prepared with 2-propanol. The respective SWNT suspensions were combined with the PP to overcoat the polymer pellets and create an initial dispersion between the polymer and the SWNTs.^{7,31,33} Then the PP pellet/SWNT suspension mixture was heated in an oil bath at temperatures between 70 and 80 °C and dried in a vacuum oven at 80 °C to completely remove the solvent. The overcoated and dried powder/pellet mixture had a gray color. The overcoated powder/pellet mixture was then compounded by high shear mixing with a HAAKE PolyLab System using a 30 cm³ mixing bowl. The material was mixed at a temperature of 165 °C for 12 min at a speed of 75 rpm. After mixing, the material was processed into pellet form before introduction into a C.W. Brabender single-screw extruder to spin the fibers. The extruder used had four independently heated zones through which the melting polymer flowed. The first zone, closest to the hopper, was heated to a temperature of 170 °C, the second was heated to 187 °C, the third was heated to 193 °C, and the fourth, at the nozzle where the material was forced through a single 0.79 mm dye, was at a temperature of 216 °C. The extruder screw was programmed to rotate at 4 rpm. The extruded material was immediately pulled onto a fiber take-up reel, which took up the fiber at a constant rate (0.422 g/min of fiber). The composite fiber diameters were measured from images taken by scanning electron microscopy (SEM) and found to be on average 130 μm . The following fibers with varying compositions were prepared:

sample type	1	neat PP
	2	2.5 wt % P-SWNT/PP
	3	5 wt % P-SWNT/PP
	4	7.5 wt % P-SWNT/PP
	5	10 wt % P-SWNT/PP
	6	2.5 wt % F-SWNT/PP
	7	5 wt % F-SWNT/PP
	8	7.5 wt % F-SWNT/PP
	9	10 wt % F-SWNT/PP

Characterization. P-SWNT and F-SWNT materials were characterized by Raman spectroscopy. A Renishaw MicroRaman spectrometer using the 780 nm diode laser with a 1200 L/m grating, 10 s exposure, and a 50 \times objective was used to depict the characteristic features expected for a spectrum of P-SWNT and F-SWNT from their respective batches. This was used to compare the state of the nanotubes after they have been incorporated into the thermoplastic matrix. The spectra indicated that some defects might have been present in the nanotubes used. There may also be amorphous carbon coating on some nanotubes or metallic catalysts still present despite any purification steps previously run on the batches by CNI. SEM imaging, Raman spectroscopy, thermogravimetric analysis (TGA), and mechanical testing were then used to evaluate the interaction between the SWNTs and PP after the processing steps. The SEM studies were performed with a Phillips Electroscan ESEM XL30 instrument. To prevent sample surface charging all composite and neat polymer samples were coated with chromium prior to analysis. The TGA experiments were conducted in air using a TA Instruments SDT 2960 device. An Instron model 5565 was used to perform the tensile tests on the fibers, following the mounting specification indicated by ASTM standard C1557-03. A 50 N load cell was used to test the samples in uniaxial tension. The gauge lengths were uniformly 25 mm; the crosshead speed used was 254 mm/min.

Results and Discussion

Sidewall functionalization considerably alters the surface morphology of the SWNTs and electronic configuration and bonding of surface carbons. The direct fluorination of the

- (26) Liu, J.; Rinzler, A. G.; Dai, H.; Hafner, J. H.; Bradley, R. K.; Boul, P. J.; Lu, A.; Iverson, T.; Shelimov, K.; Huffman, C. B.; Rodriguez-Macias, F.; Shon, Y.-S.; Lee, T. R.; Colbert, D. T.; Smalley, R. E. *Science* **1998**, *280*, 1253.
- (27) Mickelson, E. T.; Huffman, C. B.; Rinzler, A. G.; Smalley, R. E.; Hauge, R. H.; Margrave, J. L. *Chem. Phys. Lett.* **1998**, *296*, 188.
- (28) Peng, H.; Reverdy, P.; Khabashesku, V. N.; Margrave, J. L. *Chem. Commun.* **2003**, 362.
- (29) Wong, S. S.; Woolley, A. T.; Joselevich, E.; Cheung, C. L.; Lieber, C. M. *J. Am. Chem. Soc.* **1998**, *120*, 8557.
- (30) O'Connell, M. J.; Boul, P. J.; Ericson, L. M.; Huffman, C. B.; Wang, Y.; Haroz, E.; Kuper, C.; Tour, J. M.; Ausman, K.; Smalley, R. E. *Chem. Phys. Lett.* **2001**, *342*, 265.
- (31) Shofner, M. Nanotube Reinforced Thermoplastic Polymer Matrix Composites. Ph.D. Dissertation, Rice University, Houston, TX, 2003.
- (32) Geng, H.; Rosen, R.; Zheng, B.; Shimoda, H.; Fleming, L.; Liu, J.; Zhou, O. *Adv. Mater.* **2002**, *14*, 1388.
- (33) Barrera, E. V. *JOM* **2000**, *52*, 38.

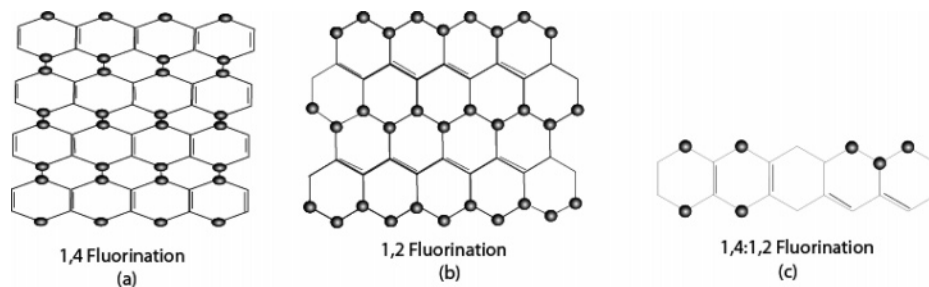
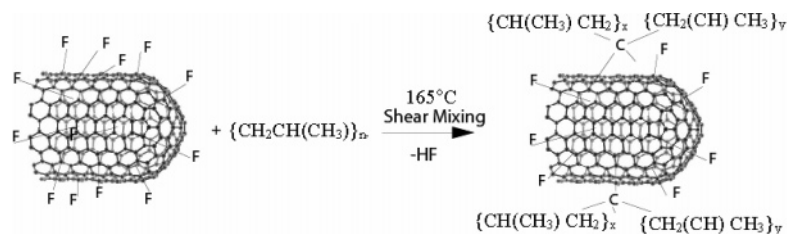


Figure 1. Patterns of fluorine addition to the sidewall of SWNT (the balls are equivalent to fluorine atom): 1,4 isomer (a), 1,2 isomer (b), and mixture of the 1,4 and 1,2 additions (c).

Scheme 1. Proposed Covalent Bonding of PP to F-SWNTs during the High Shear Mixing Processing of the PP Composite Melt



SWNTs with elementary fluorine results in the sidewall-fluorinated SWNTs (fluoronanotubes)²² where fluorine atoms were found to covalently bond in circular bands around the diameter of the nanotube reaching a saturation stoichiometry (nearly C₂F) without destruction of the tube structure, as imaged by scanning tunneling microscopy.³⁴ Molecular modeling studies predict two possible types of fluorine addition to the SWNT sidewall resulting in 1,4 and 1,2 isomers, as shown in Figure 1a,b.

However, because the calculated energy difference between the 1,2 and 1,4 isomers is very small,³⁵ it is most likely that both types of fluorine addition occur simultaneously during the fluorination process and form discrete isomeric domains on the nanotube (Figure 1c). Fluorine addition changes the bonding structure of the SWNT sidewall from polyaromatic to polyene-like with the π bonds activated by the electron withdrawing effect of fluorine substituents. The electronic configuration of a large number of sidewall carbons also transforms from the sp² to the sp³ state due to the attached fluorine. The sidewall C–F bond in fluoronanotubes is much weaker than in alkyl fluorides³⁰ and, therefore, can easier dissociate when heat and shear is applied.

These modified sidewall properties of the SWNTs were exploited in the present work to facilitate a chemical interlocking of the nanotube to the surrounding polymer matrix via the proposed mechanism shown in Scheme 1. This process facilitates a chemical interface where the PP is directly attached to the carbon nanotube allowing for better load transfer from the surrounding matrix to the stronger nanotube acting more effectively as the reinforcing element of the composite. The improvement in adhesion contributes to the tensile testing results generated. In forming these continuous fiber systems the processing steps have become

integral in achieving the improvements in the mechanical properties of the resulting composite materials. The use of high shear mixing during the processing stage not only disrupts the bundles and disperses the SWNTs throughout the polymer matrix but also initiates, under high temperature conditions, an in situ reaction very likely leading to formation of covalent bonds between the SWNT and the polymer matrix as proposed by Scheme 1.

Raman spectroscopic analysis of the pure F-SWNTs, done before (Figure 2) and after (Figure 3) their introduction into the polymer matrix, supports the possibility of a covalent bonding of the PP to the SWNTs. The disorder mode (D band) is indicative of sidewall defects arising from the sp³ carbon bonding states, and the tangential mode (G band) is indicative of the sp² C=C stretching mode. The position and peak intensity of these modes are used to evaluate the interaction between the nanotubes and the polymer. The Raman spectra of the 2.5 wt %, 5 wt %, 7.5 wt %, and 10 wt % SWNT-loaded composite systems are shown in Figure 3.

The suggested formation of covalent bonds between the carbon atoms of the PP and the nanotube, resulting from intermolecular loss of HF (Scheme 1), is supported by the observed Raman upshift of the D-band from 1291 cm⁻¹ for the pure F-SWNT (Figure 2) to 1310 cm⁻¹ for the composite system (Figure 3). The sp³ carbon Raman peak shifts to a

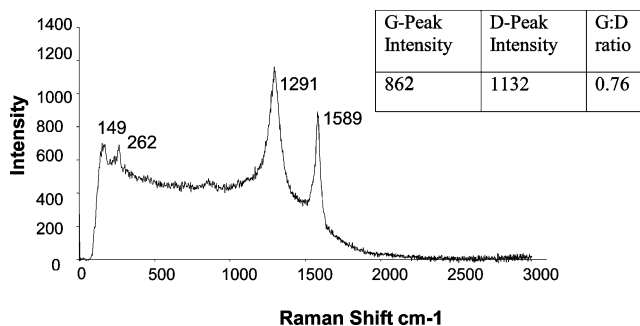


Figure 2. Raman spectra of F-SWNTs taken before incorporation into the polymer matrix.

(34) Kelly, K. F.; Chiang, I. W.; Mickelson, E. T.; Hauge, R. H.; Margrave, J. L.; Wang, X.; Scuseria, G. E.; Radloff, C.; Halas, N. J. *Chem. Phys. Lett.* **1999**, *313*, 445.

(35) Kudin, K. N.; Bettinger, H. F.; Scuseria, G. E. *Phys. Rev. B* **2001**, *63*, 45413.

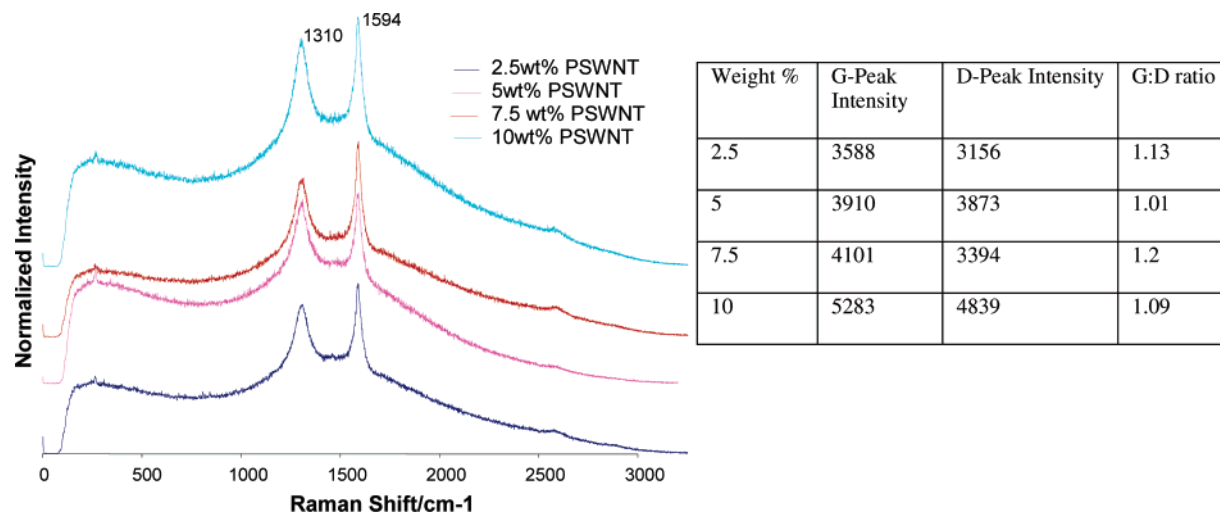


Figure 3. Raman spectra of composite samples containing varying weight percent loads of F-SWNT in the PP matrix.

higher frequency in the composite systems compared to the pure material as a result of substitution of fluorine by a lighter element, such as carbon. Fluorine is being detached with the application of high temperature and shear force during the high shear mixing process. The fluorine atoms, detached from the nanotube, are capable of scavenging hydrogen atoms from the PP matrix and form HF gas. The removal of hydrogen atoms from the chain in turn generates open radical sites on the polymer which combine with the radical sites on the F-SWNT sidewall to create new sp^3 carbon-carbon bonds grafting the PP chains to the nanotube sidewall (Scheme 1).

The substantial loss of fluorine is likely indicated by the observed decrease in Raman peak intensities of the disorder mode (D band, 1310 cm^{-1}) relative to the tangential mode (G band, 1594 cm^{-1}) in the composite systems (Figure 3) during the processing steps as compared to unprocessed F-SWNTs (Figure 2). The calculated increase in the G:D peak intensity ratios for processed composites (Figure 3) versus pure F-SWNTs (Figure 2) also shows that even after the loss of most of the fluorine moieties the nanotubes remain sidewall functionalized.

The processing of PP composites by fiber spinning also causes the alignment of the SWNTs, which have been covalently bonded into the polymer matrix due to occurrence of chemical process via Scheme 1. The degree of alignment of the nanotubes in the polymer matrix significantly affects the mechanical strength attainable by the final composite.³⁴ The alignment of the reinforcing SWNTs, in the axial direction, facilitates better utilization of the high mechanical properties of the anisotropic nanotubes or smaller ropes of nanotubes. The alignment achieved is verified with the help of polarized Raman spectroscopy which collects the spectra from the individual fibers with their fiber axis oriented either parallel (0°) or perpendicular (90°) to the incident light polarization provided by the 780 nm laser we used. Researchers including Dresselhaus et al.³⁶ and Yang et al.³⁷ used

this particular method to conduct research on aligned SWNTs and found that carbon nanotubes behave as antennas which show reduced light absorption/emission when light is polarized perpendicular to the nanotube axis. On the basis of these data, the highest Raman intensity is expected for light polarized along the tube axis (for the analyzed fibers this is the parallel (0°) orientation) and much lower signal intensities for cross polarized light (the perpendicular (90°) orientation). The resulting polarized Raman spectra of the composite fiber samples are shown in Figures 4 and 5. Aligned nanotubes, whether individual or roped, for both the P-SWNT (Figure 4) and F-SWNT (Figure 5) continuous fibers show significantly higher intensities for fibers with the fiber axis oriented parallel to the incident laser polarization. According to the data presented in Table 1, the intensity of the tangential G-mode of SWNTs in such oriented fibers is being enhanced more than the intensity of the D-mode as compared to fibers oriented perpendicular to polarized light.

The observed distinction due to the orientation effect is more prominent in the Raman spectrum of F-SWNT/PP composite continuous fibers (Figure 5). The marked increases in the ratio of the G to D peaks (Table 2) correlate to the macroscopic alignment of the SWNTs and their ropes and bundles in the fibers spun. This further supports the proposed idea of covalent bonding of the PP chain to SWNT sidewalls, taking place according to the mechanism shown in Scheme 1. Because the nanotubes are becoming attached at intervals to the polymer chains and are pulled in the direction of fiber take-up, this allows for better manipulation of the alignment of the nanotube during the drawing phase of fiber spinning.

The mechanical properties of the fabricated NCFs show improvements in strength and modulus as a result of the better interfacial adhesion and alignment that are achieved in these small diameter fibers. The results for the mechanical properties of the neat PP, P-SWNT, and F-SWNT NCFs are shown in Tables 3 and 4. The NCFs, which contain only P-SWNTs, do not show significant improvements, within the error limits, in mechanical properties over that of the neat PP fibers (Table 3). However, with the introduction of the F-SWNTs there are noticeable increases in the mechanical properties of the composite fiber system (Table 4). For these

(36) Dresselhaus, M. S.; Dresselhaus, G.; Jorio, A.; Souza Filho, A. G.; Saito, R. *Carbon* **2003**, *40*, 2043.

(37) Yang, Q. H.; Bai, S.; Fournier, T.; Li, F.; Wang, G.; Cheng, H. M.; Bai, J. B. *Chem. Phys. Lett.* **2003**, *370*, 274.

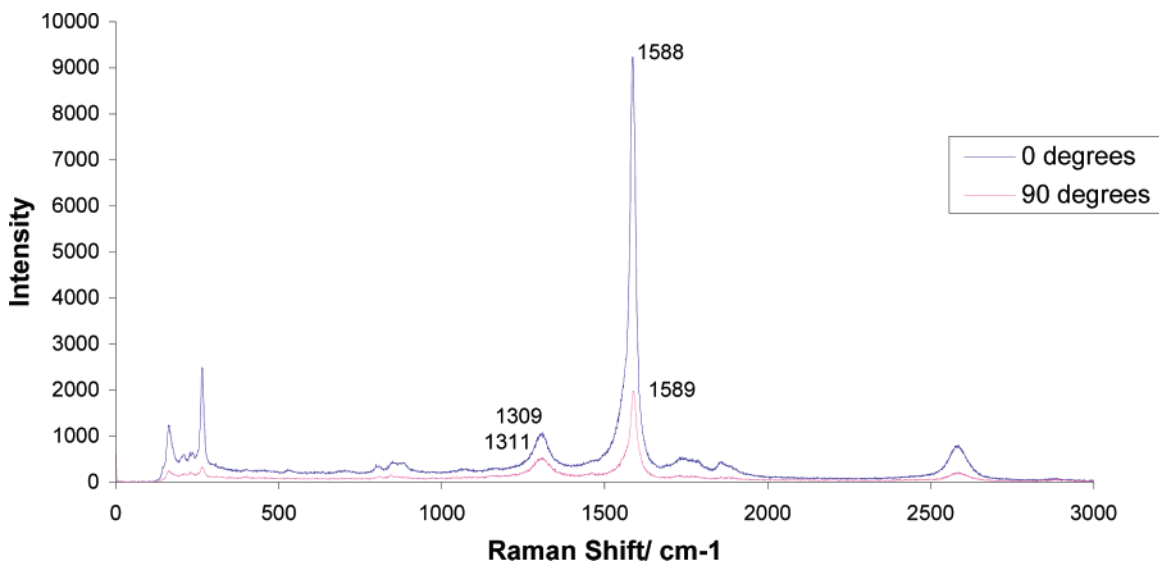


Figure 4. Polarized Raman spectra of the fiber sample made of PP with 10 wt % load of P-SWNT. Note the significant difference in the intensities of the D and G peaks.

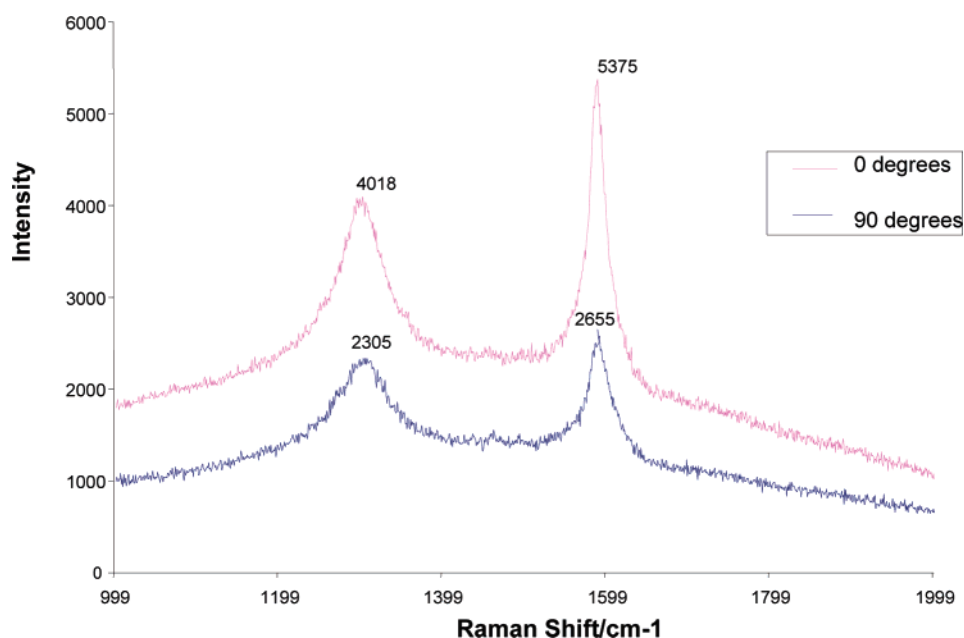


Figure 5. Polarized Raman spectra of the fiber sample made of PP with 10 wt % load of F-SWNT. Note the variations in the intensities attained with degree of alignment of F-SWNTs in PP composite fibers. Intensities, not frequencies, are identified.

Table 1. Calculated Raman Peak Intensity Ratios for 0 and 90° Oriented Fibers of P-SWNT in PP

sample	fiber-axis orientation	G-peak intensity	D-peak intensity	G:D ratio
10 wt % P-SWNT in PP fiber	0°	6664	742	8.98
	90°	2857	607	4.71
		G:G ratio	D:D ratio	
0°:90° ratio		2.33	1.22	

Table 2. Calculated Raman Peak Intensity Ratios for 0 and 90° Oriented Fibers of F-SWNT in PP

sample	fiber-axis orientation	G-peak intensity	D-peak intensity	G:D ratio
10 wt % F-SWNT in PP fiber	0°	5375	4018	1.34
	90°	2655	2305	1.24
		G:G ratio	D:D ratio	
0°:90° ratio		2.02	1.74	

systems, the F-SWNT NCFs show a 47.8, 36.3, 67.4, and 151.2% increase in tensile strength for the 2.5 wt %, 5 wt %, 7.5 wt %, 10 wt % NCFs, respectively, over that of the neat fiber, and a 31.8, 72, 65.5, and 110.5 increase in tensile modulus for the respective weight percents over the neat fiber.

The comparative results of tensile strengths, elastic modulus, and % elongation property tests are illustrated in Figures 6–8. The prepared samples show an increase in

brittleness with the increase in concentration of nanotube content for both the P-SWNT and F-SWNTs NCFs; however, the samples are still capable of achieving immense elongations as shown in Figure 8.

The mechanical properties achieved indicate that the proposed covalent attachment of the SWNT to the matrix was successful. This interlocking of the SWNTs with the surrounding polymer, in conjunction with the alignment of the molecular chains of the polymer matrix, in the small

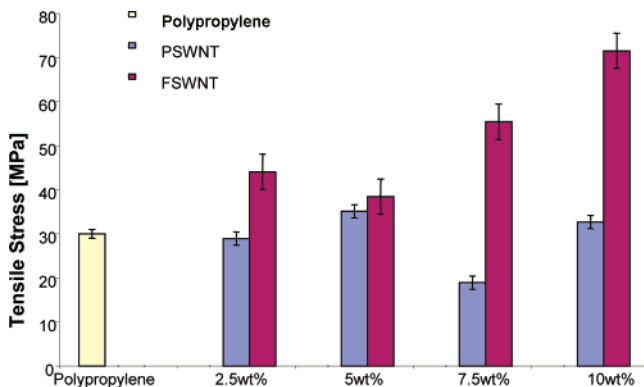
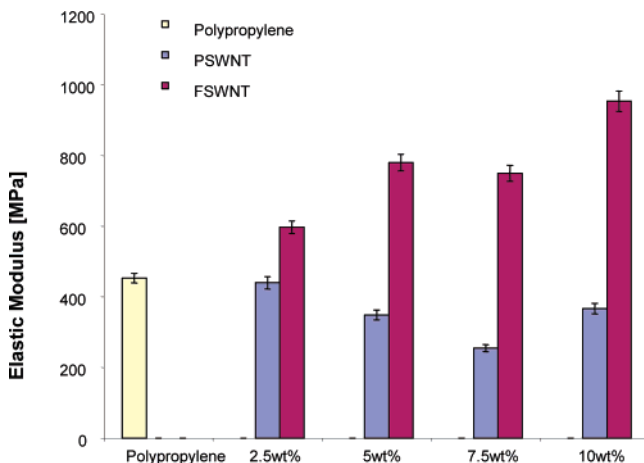
Table 3. Mechanical Properties of Neat PP Fiber and Varying Weight Percentages of P-SWNT NCFs

sample	average diameter [μm]	extension at failure [mm]	maximum stress [MPa]	tensile modulus [MPa]
neat PP	130	398 \pm 19.9	30.65 \pm 1.86	453.26 \pm 14
2.5 wt % P-SWNT	130	133.13 \pm 27	28.9 \pm 5.39	440 \pm 8.7
5 wt % P-SWNT	130	197.5 \pm 21	35.1 \pm 4.83	349 \pm 6.4
7.5 wt % P-SWNT	130	153.2 \pm 15	18.9 \pm 4.33	255 \pm 5.4
10 wt % P-SWNT	130	151 \pm 24	32.6 \pm 8.54	366.5 \pm 7.8

Table 4. Mechanical Properties of Varying Weight Percentages of F-SWNT NCFs

sample	average diameter [μm]	extension at failure [mm]	maximum stress [MPa]	increase max stress [%]	tensile modulus [MPa]	increase tensile modulus [%]
neat PP	130	398 \pm 19.9	30.65 \pm 1.86		453.26 \pm 14	
2.5 wt % F-SWNT	130	184.85 \pm 35	45.3 \pm 3.37	47.8	597.4 \pm 5.4	31.8
5 wt % F-SWNT	130	132.7 \pm 29	41.78 \pm 8.36	36.3	780.5 \pm 8.37	72.1
7.5 wt % F-SWNT	130	117 \pm 103	51.3 \pm 14.68	67.4	750 \pm 15.37	65.5
10 wt % F-SWNT	130	203 \pm 56	77.0 \pm 13.5	151.2	954 \pm 18.6	110.5

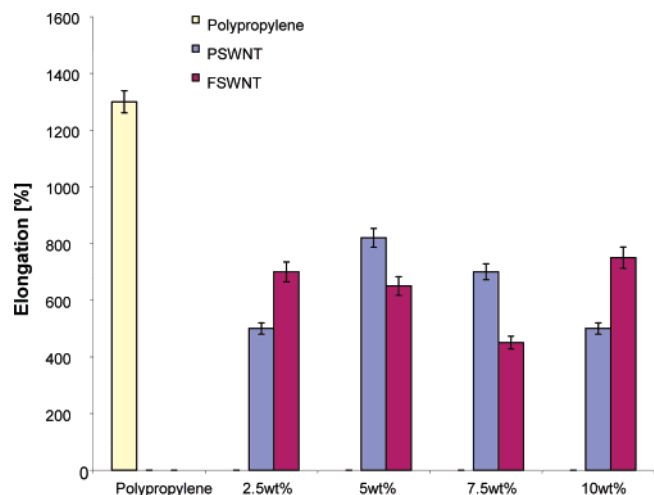
diameter fibers generated the improved mechanical properties shown in Figure 6. Not only are we taking advantage of the high crystallinity of the polymer, but by incorporating the SWNTs via the in situ reaction proposed we are creating a composite system capable of better load transfer from the matrix to the reinforcing material. Although the reaction scheme proposed to do this is seemingly effective, it is likely that the in situ reaction scheme proposed preferentially affects the exterior regions of any existing ropes of SWNTs, allowing for slippage once the exterior ropes are pulled in the direction of the applied load leading to failure. Therefore, if even better dispersion of the starting F-SWNTs material is achieved, a better composite ultimately can be generated.

**Figure 6.** Comparison of tensile strengths for 130 μm fibers.**Figure 7.** Comparison of elastic moduli for 130 μm fibers.

In evaluating other mechanical properties of the NCFs it was found that significant elongations to failure could be achieved despite the addition of carbon nanotubes, which previously were shown to contribute to the embrittlement of thermoplastic composites. The percent elongation of the NCFs we produced demonstrates that there is a decrease in the percent elongations as higher weight percents of F-SWNT are incorporated into the matrix. However, for this grade of PP we are able to achieve near 700% elongation in the worst case (10 wt % F-SWNT), which is a significant elongation in and of itself despite the decrease compared to the neat polymer.

The mechanical properties demonstrated by our NCFs prove promising and are definitely enhanced by the formation of an aligned configuration inherent to the fibers generated. The efficiency of Scheme 1 is not yet fully determined, and, therefore, the translation to a bulk system may not be as successful because one of the things exploited is the alignment of the nanotubes and polymer chains within the matrix.

SEM analysis of the fracture surfaces of the fibers tested is shown in Figures 9–11. These images reinforce the idea that there is a wrapping of the nanotubes by the surrounding polymer via Scheme 1 leading to better fiber–matrix interface and enhanced mechanical properties as a consequence of increased load transfer between the two compo-

**Figure 8.** Comparison of percent elongations for 130 μm fibers.

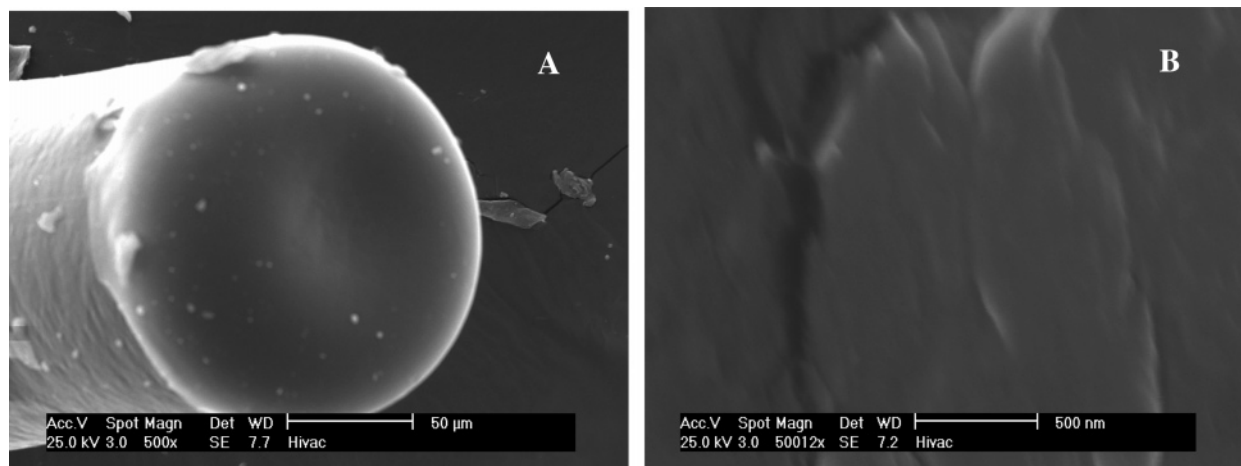


Figure 9. SEM image of the neat PP fiber fracture surface shown at lower (A) and higher (B) magnifications.

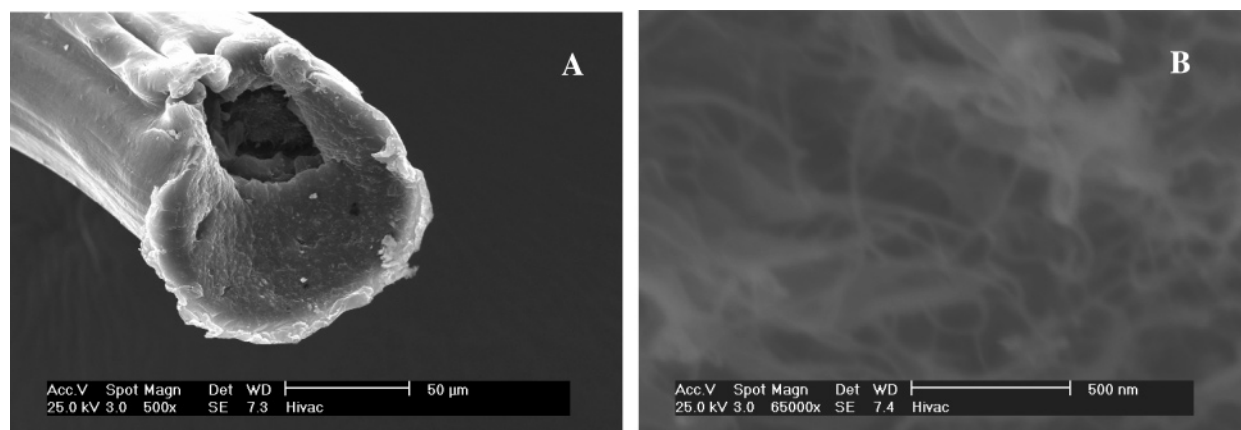


Figure 10. SEM image of the fracture surface of a NCF containing P-SWNTs shown at lower (A) and higher magnification (B) where the ropes of nanotubes have been pulled out of the matrix during fracture.

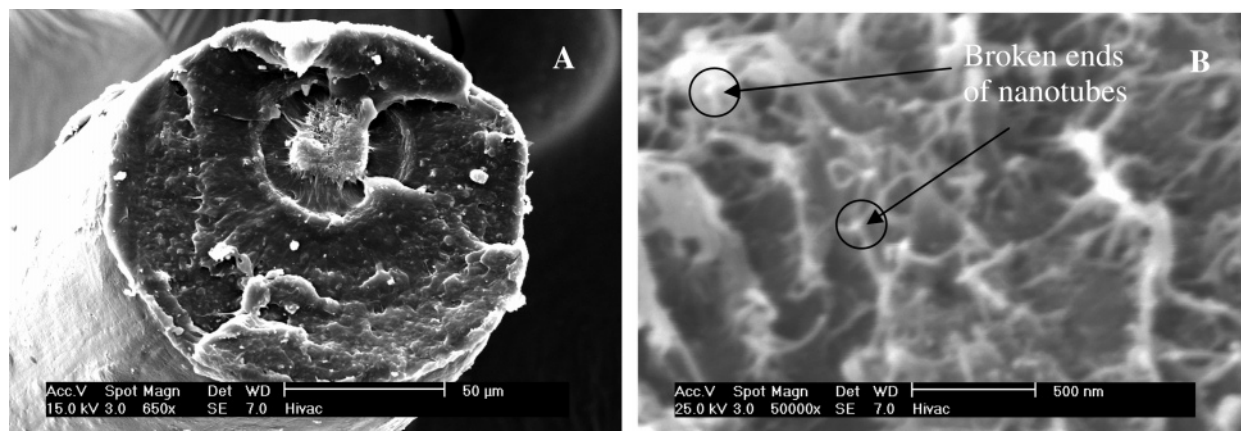


Figure 11. SEM image of the fracture surface of a NCF containing F-SWNTs shown at lower (A) and higher magnification (B). In the image B broken ends of polymer wrapped nanotubes are visible in contrast to the long spaghetti-like fiber seen for the P-SWNT in Figure 10B.

nents of the fiber. The result of this is that there is evidence of nanotube fracture, instead of pullout (Figure 10), at the point of failure of the fiber in samples where F-SWNTs had been incorporated into the polymer matrix (Figure 11) versus samples where P-SWNTs had been incorporated (Figure 10).

The fracture surfaces of the NCFs shown demonstrate that the fibers which contained F-SWNTs showed better polymer wrapping of the incorporated nanotubes even up to the point of fracture. The images of the NCFs containing F-SWNTs in Figure 11 show the fractured ends of the nanotubes at

failure in contrast to the long spaghetti-like ropes of nanotubes, indicative of rope pullout, shown in Figure 10 where less interaction with the matrix has occurred because of the incorporation of the untreated P-SWNTs. These SEM images further support the mechanical testing results shown earlier where the fibers, which incorporated P-SWNTs, showed inferior mechanical properties to those in which F-SWNTs have been incorporated. The images show that the NCFs containing F-SWNTs had better a matrix–nanotube interface and, therefore, were able the support better

load transfer leading to nanotube fracture instead of pullout, facilitating the higher mechanical properties previously shown.

Conclusions

The fabrication of continuous PP/F-SWNT composite fiber systems produced fibers which, because of better adhesion, demonstrate improved interfacial and alignment characteristics that have in concert led to improved mechanical properties. In using F-SWNTs, the sidewall fluorine moieties not only disrupt the nanotube rope structure facilitating better dispersion but also provide sites for possible direct covalent bonding of the nanotube to the PP matrix via an in situ high temperature initiated reaction. This work demonstrates a fabrication method for NCFs that is based on easily processed composite materials which can be easily used in conventional processing technologies.

The proposed method of formation of a fully integrated composite system through incorporation of SWNTs uses free radical initiated reactions with the surrounding polymer matrix occurring during processing. The suggested covalent

bonding of the SWNTs to the polymer provides not only for a more effective use of SWNTs as the reinforcing material but also presents the possibility for the synthesis of an entirely new graft copolymer type material. Nanotubes soon can be surface tailored to function as initiators for particular polymerization reactions that will result in a more seamless pairing of the reinforcement material (SWNTs) with the surrounding polymer matrix. The advantage of this approach will be in better manipulation of nanotube dispersion to allow a more efficient exploitation of the mechanical properties of the SWNTs and produce completely new classes of materials that can be used for multiple purposes ranging from electrical through mechanical applications.

Acknowledgment. This research was funded by the Welch Foundation Grant C-1494, and NASA Cooperative Agreement NCC-1-02036, and the Texas ATP Grant 003599-0010. The authors also thank Dr. Felipe Chibante, of NanoTex Corporation, for providing access to his facilities for the preparation of fiber samples.

CM060513Q